Common explanation of the behavior of some e^+e^- annihilation processes around $\sqrt{s} = 1.9$ GeV

Peter Lichard

Institute of Physics and Research Centre for Computational Physics and Data Processing,
Silesian University in Opava, 746 01 Opava, Czech Republic
and
Institute of Experimental and Applied Physics,
Czech Technical University in Prague,
128 00 Prague, Czech Republic

We show that the behavior of the excitation curves of some e^+e^- annihilation processes close to the nucleon-antinucleon threshold can be explained either by the $\rho(1900)$ resonance itself or by its interference with other resonances. Besides the six-pion annihilation and the $e^+e^- \to K^+K^-\pi^+\pi^-$ and $e^+e^- \to \phi\pi^0$ processes, we also analyze the final states $\eta\,\pi^+\pi^-$, $K^+K^-\pi^+\pi^-\pi^0$, and $K^+K^-\pi^0\pi^0$, the behavior of which around 1.9 GeV has not yet attracted attention. Analysis of the data on the $e^+e^- \to p\bar{p}$ and $e^+e^- \to n\bar{n}$ reactions clearly shows that the $\rho(1900)$ resides above the $n\bar{n}$ threshold.

I. INTRODUCTION

Interesting phenomena have been observed in many experiments when the invariant energy $\sqrt{s}$ of the final system or its subsystem reaches the vicinity of 1.9 GeV (which is the energy very close to the $N\bar{N}$ thresholds). The aim of this work is to show that all such phenomena have their origins in the existence of the narrow ρ-like resonance $\rho(1900)$. It has not found its way into the Particle Data Group (PDG) [1] Summary Tables, but is mentioned in their Particle Listings.

Most of the data pointing to the role of the $\rho(1900)$ resonance are the cross section for the e^+e^- annihilation into various final states. This is the class of processes we will concentrate on in this work. The examples of other processes are the photoproduction of mesonic systems and the decays of quarkonia and heavy mesons.

The hints about a possible role of the $\rho(1900)$ resonance in the e^+e^- annihilation into various final states have appeared in the papers by the Novosibirsk theory group [2–4]. But the limited accuracy of the data they fitted allowed only vague determination of the resonance parameters and did not reveal detailed behavior of the cross section in the vicinity of $\sqrt{s} = 1.9$ GeV.

The tools we use when fitting the cross section data to various processes and determining the parameters of resonances are the models described in Section II. For the final states with more than four particles we use the statistical (phase-space) model. Otherwise we use models based on the interaction Lagrangians pertinent for a particular process. All models are supplemented with the Vector Meson Dominance (VMD) hypothesis [5] specifying the coupling of the hadronic system to the virtual photon.

We also analyze data in which the authors already found optimal resonance parameters. Our endeavor is to describe using the same model the data coming from various experiments, so we are better able to compare their results.

Let us mention several experiments in which special

behavior around 1.9 GeV has been observed.

In the 1980s the magnetic detector experiments DM1 and DM2 at the Orsay storage ring DCI investigated the e^+e^- annihilation into six pions. The $e^+e^- \to 3(\pi^+\pi^-)$ cross section measured by the DM1 detector was published in 1981 [6]. A later experiment, DM2 investigated the $3(\pi^+\pi^-)$ and $2(\pi^+\pi^-\pi^0)$ final states, where the authors discovered a dip at about 1.9 GeV. Unfortunately, their data have not been published in any journal. They became a part of the thesis by M. Schioppa [7] and were included in the compilation by M.R. Whalley [8]. They were also presented at a meeting in 1988 [9]. The combined data from the DM1 and DM2 experiments were used in a paper by Clegg and Donnachie [10]. The salient feature of the excitation curve (Fig. 2 in [10]) is a narrow dip at $\sqrt{s} \approx 1.9$ GeV. The authors of [10] explained this structure as a consequence of the separation of two peaks formed by two (for some reason) non-interfering resonances. The quality of the fit depended on the assumed isospin symmetry states in the $3(\pi^+\pi^-)$ and $2(\pi^+\pi^-\pi^0)$ processes. The best fit was characterized by $\chi^2 = 58.0$ for the number of degrees of freedom (NDF) equal to 46, which implies a confidence level (C.L.) of 11.0%. We will show in Sec. III A 4 that a much better fit quality is achieved if the dip is described as a result of the destructive interference of a narrow resonance with a broader resonance. The parameters of the narrow resonance qualify it as the $\rho(1900)$. The latter is known from several experiments, which will be listed and analyzed in Sec. III.

In 1994, a dedicated experiment performed at the Low Energy Antiproton Ring (LEAR) at CERN [11] determined the electromagnetic proton form factors by measuring the total and differential cross sections of the reaction $p\bar{p} \to e^+e^-$. A steep s-dependence of the form factors close to the threshold was found.

The existence of a narrow resonance with a mass close to the $N\bar{N}$ threshold was suggested by the FENICE Collaboration working at the Frascati e^+e^- storage ring ADONE in 1991-93. They explained [12] in a paper

published in 1996 that such a resonance interfering with the background given by broad resonances can generate a dip in the multihadronic cross section just below the $N\bar{N}$ threshold, which they observed. Two years later, the steep rise of the proton form factor was attributed to the same resonance [13]. FENICE's estimate of the resonance parameters was $M = (1.87 \pm 0.01)$ GeV, $\Gamma = (10 \pm 5)$ MeV.

In 2001, the E687 Collaboration working at FNAL discovered a narrow dip structure in the $3\pi^+3\pi^-$ diffractive photoproduction on a Be target [14]. Later on, the E687 data were refitted and the parameters of the resonance producing the dip by the destructive interference were specified more precisely [$M = (1910 \pm 10)$ MeV, $\Gamma = (37 \pm 13)$ MeV] [15].

The *BABAR* experiment [16] (re)discovered the dip in the cross sections of the $e^+e^- \to 3(\pi^+\pi^-)$ and $e^+e^- \to 2(\pi^+\pi^-\pi^0)$ processes in 2006 and determined the parameters of the resonance which generates them. The details will be given in Sec. III A.

The cross section of the process $e^+e^- \to \phi\,\pi^0$ appeared among other results from the *BABAR* experiment in Ref. [17] published in 2008. It is special in the respect that here the $\rho(1900)$ resonance is visible as a clear isolated peak. In Sec. III B we present the results of *BABAR*'s and our fits together with their graphical representation.

In 2012, the *BABAR* Collaboration completed their $e^+e^- \to K^+K^-\pi^+\pi^-$ program, which started in 2005 [18] and continued in 2007 [19]. In [20] they presented the excitation curve in which a dip at $\sqrt{s} = 1.9$ GeV is visible. Our analysis in Sec. III E 1 shows that the data does not require the involvement of $\rho(1900)$, but can accommodate it.

In 2013, the CMD-3 experiment [21] confirmed the existence of a sharp drop of the $e^+e^- \to 3(\pi^+\pi^-)$ cross section near the $p\bar{p}$ threshold. In Sec. III A 1 we show that their result can also be explained as a manifestation of the $\rho(1900)$ resonance.

The idea that negative discontinuity in the cross section of the $e^+e^- \to 6\pi$ processes at the $N\bar{N}$ threshold can be explained by the opening of annihilation channel $e^+e^- \to N\bar{N}$ appeared in Ref. [22]. A more detailed attempt to understand the origin of the structures observed in e^+e^- annihilation into multipion states as a $p\bar{p}$ threshold effect was published in 2015 [23]. An optical potential describing simultaneously the experimental data for $N\bar{N}$ scattering and e^+e^- annihilation to $N\bar{N}$ and 6π close to the threshold of $N\bar{N}$ was proposed in Ref. [24].

The CMD-3 experiment [25] in 2016 measured the cross section of the process $e^+e^- \to K^+K^-\pi^+\pi^-$. No conspicuous dip is visible in the data, but we show in Sec. III E 2 that a better fit is achieved if the $\rho(1900)$ is taken into consideration.

Three important experiments have appeared that measured the cross section of $e^+e^- \to N\bar{N}$ at small energies: *BABAR* [26], SND [27], and CMD-3 [28]. They will be analyzed in Sec. III G by means of a simple and transparent cross section formula that follows from the ρNN

and $\gamma\rho$ Lagrangians supplemented with the VMD. They show in unison that the $\rho(1900)$ resonance lies above the $n\bar{n}$ threshold.

A very recent contribution to the arXiv [29] reports on new more precise measurements of the $e^+e^- \to 3(\pi^+\pi^-)$ and $e^+e^- \to K^+K^-\pi^+\pi^-$ cross sections. The group working on the CMD-3 experiment claim that the behavior of these cross sections cannot be explained by the interference of any resonance amplitude with continuum. They have not published their data yet, so we can neither confirm nor question their claim. The authors also stressed the correlation of the observed drops with the $p\bar{p}$ and $n\bar{n}$ threshold. We only remind that the correlation does not always mean causality.

The processes, the behavior of which in the vicinity of 1.9 GeV have not yet been investigated, are analyzed in Sections III C, III D, and III F.

II. MODELS

A. Statistical model

For the processes with more than four mesons in the final state we will evaluate the cross section using the statistical model combined with the VMD

$$\sigma = \frac{1}{8s}|V_0(s)|^2 \int (2\pi)^4 \delta^4(P - \sum_{i=1}^{n} p_i)\, \mathrm{d}\Phi_n, \quad (1)$$

where

$$\mathrm{d}\Phi_n = \prod_{i=1}^{n} \frac{\mathrm{d}^3 p_i}{(2\pi)^3\, 2E_i} \quad (2)$$

is an element of n-body phase space, and

$$V_0(s) = \frac{1}{s}\sum_i \frac{r_i \exp\{\mathrm{i}\delta_i\}}{s - M_i^2 + \mathrm{i}M_i\Gamma_i} \quad (3)$$

is the photon propagator multiplied by the sum of the propagators of the neutral vector-meson resonances. We can put $\delta_1 = 0$. The other δ's will be considered together with all r's, M's, and Γ's as free parameters.

The vector-meson propagators in (3) are chosen in a simplified form, with constant decay widths and masses. It is known [2, 4, 30] that the inverse propagator of a resonance acquires boundary values of an analytic function the imaginary part of which is proportional to the total decay width. Its real part is given by the dispersion relation that follows from the unitarity.

Our formula (3) is thus an approximation, which can be theoretically justified only for very narrow resonances. But, as the comparison with publicly available data shows, it works well. If the disagreement with data appears in the future, a more correct formalism describing the propagators of the resonances and also mixing of them [31] will have to be considered.

As we will show, the statistical model is quite successful in describing the data. The reason probably lies in the large number of possible intermediate states. The number of the corresponding Feynman diagrams is further multiplied by the exchanges of all identical mesons in the final state. When squaring the reaction amplitude, we also get, besides the quadratic terms, many interference terms and the details of dynamics are smudged. So, replacing the amplitude squared by a constant is in this case a good approximation. The only non-trivial dynamics is then represented by the VMD.

B. Lagrangian-based models

For the processes with fewer than five hadrons in the final state considered in this paper it is always possible to identify the dominant intermediate state on the basis of the conservation laws and experimental results. Then the process can be described by a single Feynman diagram, which is doubled if the identical boson symmetrization requires so. The standard Lagrangians (a useful survey of them can be found, for example, in Ref. [32]) are used to evaluate the sum of the amplitudes squared over the spin states of the initial and final particles. This sum is then inserted after the integration sign in Eq. (1). The product of coupling constants can be absorbed into the parameters r_i in Eq. (3).

The quality of the fit is sometimes improved if an exponential cutoff is applied

$$F_{KI}(s) = \exp\left\{-\frac{s - s_0}{48\beta^2}\right\}, \qquad (4)$$

where s is the square of the total invariant energy and s_0 is its threshold value. This cutoff is motivated by the results of the chromoelectric flux-tube breaking model of Kokoski and Isgur [33], according to which the strong interaction vertices are modified by an energy-dependent cutoff. Instead of applying the cutoff to each vertex, we introduce, similarly to [34], a global cutoff (4). We consider $\beta_I = 1/\beta$ as a free parameter when fitting the excitation curve of a particular process.

The exponential cutoff is a phenomenological tool which mimics the decrease of the strong coupling constants with the increasing momentum transfer squared, as expected on the basis of results of the perturbative quantum chromodynamics. In some cases it may become counterproductive, as shown in Ref. [35].

C. Computing details

A substantial part of our computer codes, written in `Fortran`, is the numerical minimization program `MINUIT` [36] from the former CERN program library, which is available now in most of the current `Linux` distributions. The errors of the parameters that result from

the fits to data are the parabolic errors defined in [36]. The phase-space integrals are evaluated by using the routine `GENBOD` [37] from the former CERN library, rewritten to double precision and furnished with a contemporary random number generator. The algebraic manipulation program `REDUCE` [38] was used to get the sum of the amplitudes squared in the Lagrangian-based models.

III. EXPERIMENTS, FITS, AND RESONANCES

A. Six-pion final states

1. $3(\pi^+\pi^-)$ in the CMD-3 experiment

The clearest indication of the steep decrease of the $e^+e^- \to 3(\pi^+\pi^-)$ cross section near the $p\bar{p}$ threshold has been provided by the CMD-3 (Cryogenic Magnetic Detector) experiment at the VEPP-2000 e^+e^- collider in Novosibirsk [21]. Recently, its original results have been confirmed by more precise and detailed measurements [29]. Unfortunately, the new data are not publicly available yet. For that reason we have made a fit to the previous data [21] using a statistical model combined with the VMD, as described in Sec. II. We show that a very good fit can be achieved, see Fig. 1, when three resonances, namely, $\rho(770)$, $\rho(1700)$, and $\rho(1900)$ are taken into ac-
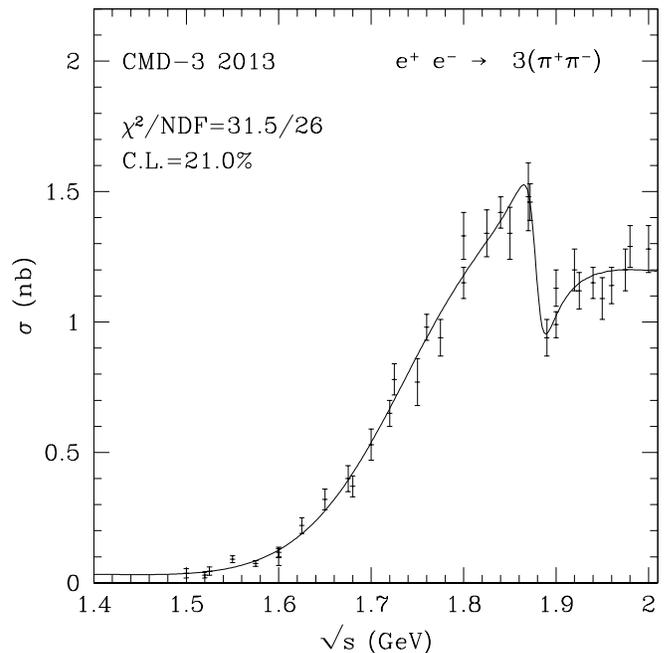

FIG. 1. Cross section for the e^+e^- annihilation into six charged pions measured in the CMD-3 experiment [21] and the fit by the statistical VMD model with three resonances.

count. The parameters of the $\rho(770)$ were taken from the PDG tables [1]. For the $\rho(1700)$ we have obtained $M = (1728 \pm 24)$ MeV, $\Gamma = (373 \pm 27)$ MeV, in agreement with [1]. The $\rho(1990)$ is not shown in the PDG [1]

Summary Tables. It is only listed in the Particle Listings, where no recommended parameters are provided. Our values $M = (1878.3 \pm 5.3)$ MeV, $\Gamma = (24.7 \pm 8.7)$ MeV agree with the values coming from various experiments shown there. To enable anybody to check that the dip in the CMD-3 data [21] shown in Fig. 1 is really caused by the interference of the $\rho(1900)$ with other resonances, we provide all the necessary parameters in Table I.

i	r_i	M_i (GeV)	Γ_i (GeV)	δ_i
1	-675.84	1.8783	0.024704	0
2	55649	1.7279	0.37265	-0.16059
3	79210	0.77526	0.14910	-1.3665

TABLE I. Parameters of the fit to the CMD-3 data [21] depicted in Fig. 1. For the statistical model with $n = 6$, the parameters r_i in Eq. (3) are dimensionless.

2. $3(\pi^+\pi^-)$ in the BABAR experiment

The drop of the $e^+e^- \to 3(\pi^+\pi^-)$ cross section close to $\sqrt{s} = 1.9$ GeV was previously seen in older data by the BABAR experiment [16], which was located at the PEP-II e^+e^- collider in the SLAC National Accelerator Laboratory. The experiment exploited the initial-state-radiation (ISR) events to measure low-energy cross section without changing the e^+e^- collider energy [39]. The BaBar detector ceased operation on 7 April 2008, but data analysis is ongoing.

To fit the BABAR data [16] we again use the VMD modified statistical model. A good fit, depicted in Fig. 2 by dashes, is already obtained with two resonances, $\rho(1700)$ and $\rho(2150)$. The quality of the fit is characterized by the χ^2/NDF = 39.0/45 and the confidence level (C.L.) of 72.3 per cent. The inclusion of the $\rho(1900)$ resonance further improves the fit, leading to χ^2/NDF = 29.1/41 and C.L.=91.8% (solid curve in Fig. 2). Its parameters come out as $M = (1884 \pm 29)$ MeV, $\Gamma = (72 \pm 39)$ MeV.

3. $2(\pi^+\pi^-\pi^0)$ in the BABAR experiment

In the same publication [16], the BABAR experiment also presented the results on the excitation curve of the process $e^+e^- \to 2(\pi^+\pi^-\pi^0)$, see Fig. 3. We made a similar analysis as in the previous six-charged-pion case. A good description (χ^2/NDF = 28.7/45, C.L.=97.2%) of the data is provided by the statistical VMD model with the $\rho(1700)$ and $\rho(2150)$ resonances (dashed curve in Fig. 3). Again, adding the $\rho(1900)$ resonance improves the quality of the fit, but here only very marginally (χ^2/NDF = 24.2/41, C.L.=98.3%, solid curve). Given this, the outcome of the $\rho(1900)$ mass (1896 ± 60) MeV and width (53 ± 58) MeV must be taken with reservation.
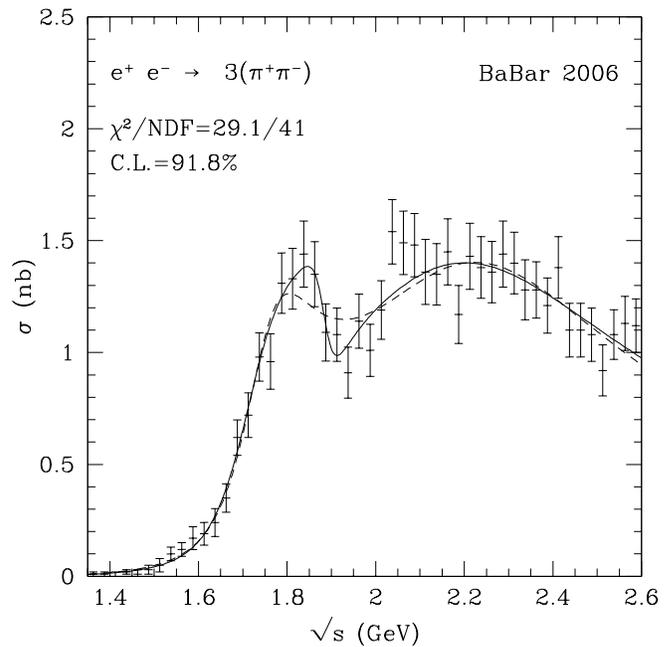

FIG. 2. Cross section for the e^+e^- annihilation into six charged pions measured in the BABAR experiment [16] and the fit by the statistical VMD model with two (dashed curve) and three resonances (solid curve).

4. Dip at 1.9 GeV in the DM2 $2(\pi^+\pi^-\pi^0)$ data

The data we have obtained from Ref. [8] are depicted in Fig. 4 together with our two-resonance fit by the VMD modified statistical model. The narrow dip at about 1.9 GeV is caused by the destructive interference of the $\rho(1900)$ resonance with the background provided by the other resonance. The quality of the fit is excellent: χ^2/NDF = 16.4/37, C.L.=99.9%. The $\rho(1900)$ resonance parameters $M = (1878 \pm 40)$ MeV, $\Gamma = (126 \pm 92)$ MeV agree with those from the other experiments presented in this Section.

5. Dip at 1.9 GeV in the DM2 $3(\pi^+\pi^-)$ data

The data are shown in Fig. 5 together with our two-resonance fit by the VMD-modified statistical model. The narrow dip at about 1.9 GeV is a result of the destructive interference of the $\rho(1900)$ resonance with the accompanying resonance. The quality of the fit is worse than in the $2(\pi^+\pi^-\pi^0)$ case: χ^2/NDF = 35.1/23, C.L.=5.1%. The $\rho(1900)$ resonance parameters coming from the fit are $M = (1888 \pm 18)$ MeV and $\Gamma = (44 \pm 37)$ MeV.
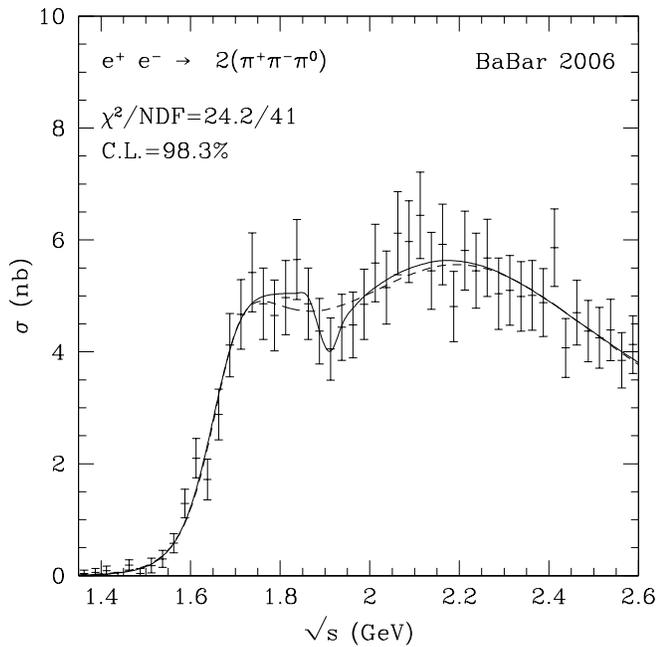
FIG. 3. Cross section for the e^+e^- annihilation into four charged and two neutral pions measured in the *BABAR* experiment [16] and the fit by the statistical VMD model with two (dashed curve) and three resonances (solid curve).

B. Peak in the $e^+e^- \to \phi\pi^0$ process

The data about this process were published by the *BABAR* Collaboration in 2008 [17]. The cross section for this process is very small because the $\rho^0\phi\pi^0$ vertex is suppressed by the Okubo–Zweig–Iizuka (OZI) rule [40]. In comparison with the cross section for a similar two-body OZI allowed process $e^+e^- \to \omega\pi^0$ [41] it is smaller by almost two orders of magnitude. For us, this process is extremely interesting because it is one of the known processes where the $\rho(1900)$ manifests itself as a narrow peak in the excitation curve, see Fig. 6. The other such processes will be dealt with in Sec. III G.

In Table II we present the results of the fit obtained by the *BABAR* Collaboration [17] together with the results of our Lagrangian-based VMD model (the cross section formula is given in Appendix). The excitation curves that correspond to those two fits are depicted in Fig. 6. Our results agree with those obtained by S. Pacetti [42],

	BABAR 2008	Our fit
M_1 (MeV)	1570 ± 36	1573 ± 25
Γ_1 (MeV)	144 ± 75	88 ± 48
M_2 (MeV)	1909 ± 17	1906.7 ± 8.8
Γ_2 (MeV)	48 ± 17	38 ± 52
χ^2/NDF	$7.37/8$	$6.7/7$
C.L.	50%	47.3%

TABLE II. Parameters of the fit to the $e^+e^- \to \phi\pi^0$ data [17] obtained by the *BABAR* Collaboration compared to the results of our fit.
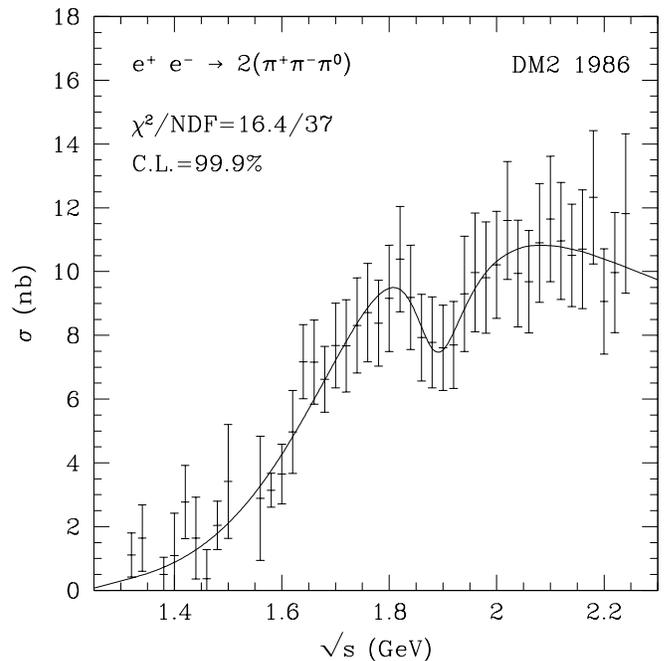

FIG. 4. The data from the DM2 experiment at Orsay [8] and our two-resonance fit.
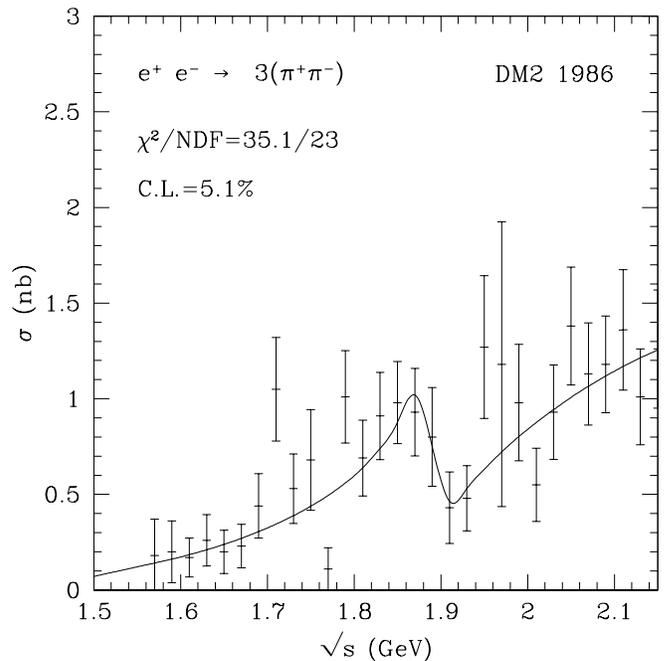

FIG. 5. The data from the DM2 experiment at Orsay taken from Ref. [8] and our two-resonance fit.

who used the transition form factor method.

A natural question arises why the $\rho(1900)$ shows here as a bright peak without interference with any reso-
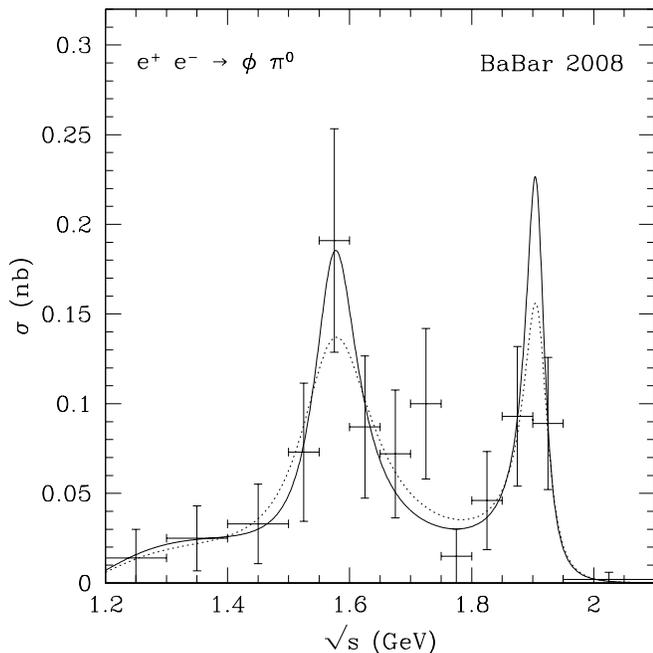
FIG. 6. Cross section for the e^+e^- annihilation into the $\phi(1020)$ and π^0 measured by the *BABAR* Collaboration [17] and the fit by our model (solid curve) and the fit using the resonance parameters determined by the *BABAR* Collaboration (dashed curve) shown it Table II.

nance.[1] The answer is that because of the isospin-one character of the final state, the intermediate resonances with zero isospin (ω-like and ϕ-like) are suppressed and the nearest ρ-like resonance [$\rho(1700)$] does not couple to the $\phi\pi^0$ system [1].

The process $e^+e^- \to \phi\pi^0$ is more convenient for the study of the $\rho(1900)$ resonance than, for example, the reaction $e^+e^- \to K^+K^-\pi^0$. In the latter, which was presented in the same paper [17], the intermediate state $\rho \to \phi\pi^0$ is also present. But it is OZI suppressed in comparison with the dominant intermediate states $\phi(1680) \to K^+K^{*-}$ and $\phi(1680) \to K^{*+}K^-$. All three intermediate states lead to the same final state $K^+K^-\pi^0$, so the interference among them is inevitable. This gives a chance that in a more precise experiment the $\rho(1900)$ will show up also in $e^+e^- \to K^+K^-\pi^0$.

C. Cross section drop in the $e^+e^- \to \pi^+\pi^-\eta$

For the purpose of fitting the data on this process we have prepared a simple model reflecting the notion that the $\rho\eta$ is the dominant intermediate state. It is based on the standard $\rho\eta\rho'$ and $\rho\pi\pi$ Lagrangians.

There are four papers that have reported on the cross section of the process $e^+e^- \to \pi^+\pi^-\eta$. Two of them

---

[1] I thank Dr. Juráň for his initiating the discussion.

[43, 44] came from the Spherical Neutral Detector (SND) experiment at the VEPP-2000 e^+e^- collider in Novosibirsk, the other two [45, 46] were published by the *BABAR* Collaboration.

1. $\eta \pi^+\pi^-$ in the SND experiments

The SND experiment obtained data in the $\eta \to \gamma\gamma$ [43] and $\eta \to 3\pi^0$ decay modes [44]. The two sets have been found to be in agreement and therefore analyzed together in [44]. Also here, we fit the combined set of data, which contains 72 data points. If we assume two resonances, we get a very nice agreement with data ($\chi^2/\text{NDF} = 44.3/64$, C.L.=97.1%), see the dotted curve in Fig. 7. If we also
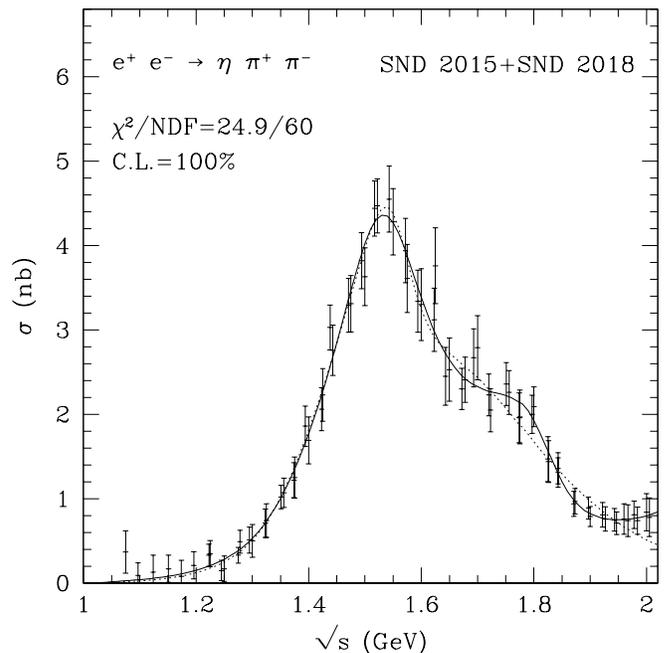

FIG. 7. Cross section for the $e^+e^- \to \eta \pi^+\pi^-$ process measured by the SND Collaboration [43, 44] and the fit by the Lagrangian VMD model with two (dotted curve) and three resonances (solid curve).

include the third resonance in our model, χ^2 drops from 44.3 to 24.9, which together with the NDF = 60, means a confidence level of 100 per cent. The new fit is depicted by a solid curve in Fig. 7. This curve exhibits a drop in the proximity of the nucleon-antinucleon threshold. The following resonance parameters come out:

$$M_1 = (1533 \pm 21) \text{ MeV} \quad \Gamma_1 = (203 \pm 43) \text{ MeV}$$
$$M_2 = (1812 \pm 31) \text{ MeV} \quad \Gamma_2 = (162 \pm 70) \text{ MeV}$$
$$M_3 = (2220 \pm 172) \text{ MeV} \quad \Gamma_3 = (3 \pm 140) \text{ MeV}$$

The middle resonance, by its parameters, is similar to $\rho(1900)$. But because the data are also well fit by two resonances, our three-resonance result cannot be considered as proof of either the rapid drop existence or the role of the $\rho(1900)$ in this process.

2. η π⁺π⁻ in BABAR 2007

The *BABAR* Collaboration in their publication [45] identified the η resonance by its $\pi^+\pi^-\pi^0$ decay mode. Our two-resonance fit with $\rho(1450)$ and $\rho(2150)$, shown in Fig. 8 by dots, leads to $\chi^2/\mathrm{NDF} = 26.6/24$ (C.L.=
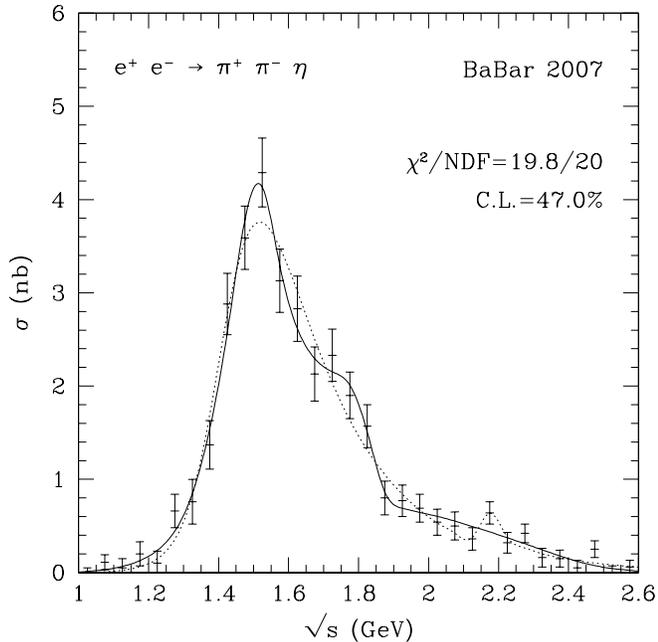

FIG. 8. Cross section for the $e^+e^- \to \eta\,\pi^+\pi^-$ process measured by the *BABAR* Collaboration [45] and the fit by the Lagrangian VMD model with two (dotted curve) and three resonances (solid curve).

32.3%). After assuming the third resonance, χ^2 drops to 19.8, the confidence level improves to 47%, and the drop close to the $N\bar{N}$ threshold becomes more visible (solid curve). The third resonance parameters are $M = (1831 \pm 48)$ MeV and $\Gamma = (146 \pm 167)$ MeV, which identifies it as the $\rho(1900)$.

3. η π⁺π⁻ in BABAR 2018

In a very recent paper by the *BABAR* Collaboration [46] the $\eta \to \gamma\gamma$ mode has been utilized. The results are in agreement with their previous result in the independent $\eta \to \pi^+\pi^-\pi^0$ channel [45]. The rapid drop of the excitation curve below $\sqrt{s} = 1.9$ GeV is already evident in their data by the naked eye, see Fig. 9. The *BABAR* Collaboration fit their data with four different models, each in its own invariant energy range. The widest energy range, up to $\sqrt{s} = 2.2$ GeV, is covered by their Model 4, which used the VMD with four resonances [$\rho(770)$ mass and width were fixed at the PDG values]. To facilitate the comparison with their fit results, we choose the same energy range.

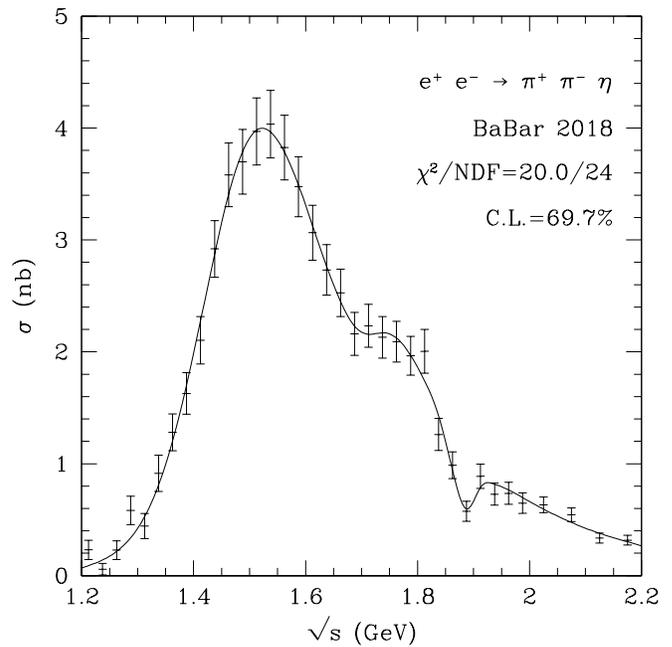Our fit with three resonances yields $\chi^2/\mathrm{NDF} =$

FIG. 9. Cross section for the $e^+e^- \to \eta\,\pi^+\pi^-$ process measured by the *BABAR* Collaboration [46] and the fit by the Lagrangian VMD model with three resonances.

20.0/24, C.L.=69.7%, see the solid curve in Fig. 9. The quality of the fit is even better than that of *BABAR*'s four-resonance fit ($\chi^2/\mathrm{NDF} = 28/26$, what means the C.L. of 36%). The obtained masses and widths of the resonances are

$$M_1 = (1461 \pm 30)\ \mathrm{MeV} \quad \Gamma_1 = (371 \pm 51)\ \mathrm{MeV}$$
$$M_2 = (1725 \pm 63)\ \mathrm{MeV} \quad \Gamma_2 = (159 \pm 137)\ \mathrm{MeV}$$
$$M_3 = (1879 \pm 10)\ \mathrm{MeV} \quad \Gamma_3 = (54 \pm 28)\ \mathrm{MeV}.$$

Obviously, these are the $\rho(1450)$, $\rho(1700)$, and $\rho(1900)$ resonances. The shape of the drop could be described even better if we took a model with four resonances. But then we would get two resonances with very close masses (1836 and 1883 MeV). This we deem artificial and unphysical.

D. Cross section jump in the $e^+e^- \to K^+K^-\pi^+\pi^-\pi^0$ process

Another interesting phenomenon that has escaped attention until now concerns the cross section of the process $e^+e^- \to K^+K^-\pi^+\pi^-\pi^0$ measured by the *BABAR* Collaboration in 2007 [45]. The initial rise above the threshold is a little below $\sqrt{s} = 1.9$ GeV interrupted by a narrow dip followed by a very rapid increase, after which the previous trend is restored, see Fig. 10.

The behavior just described can be perfectly ($\chi^2/NDF = 23.6/32$, C.L.= 85.8%) reproduced by the VMD-modified statistical model with two resonances, see the solid curve. One of them is again the $\rho(1900)$, the
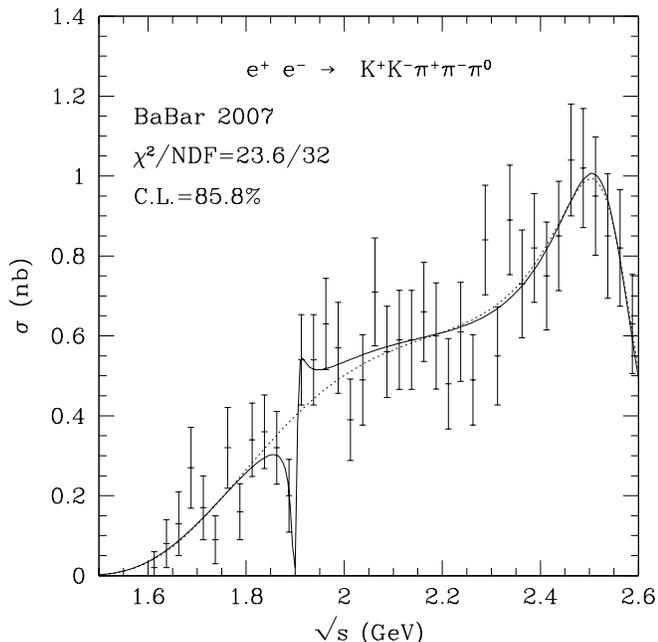
FIG. 10. Cross section for the $e^+e^- \to K^+K^-\pi^+\pi^-\pi^0$ process measured by the *BABAR* Collaboration [45] and the fits using the statistical VMD model with two resonances (solid curve) and one resonance (dotted curve).

parameters of which come out as $M_1 = (1902 \pm 26)$ MeV, $\Gamma_1 = (11 \pm 20)$ MeV. The other resonance is characterized by $M_2 = (2550 \pm 13)$ MeV, $\Gamma_2 = (209 \pm 26)$ MeV.

It must be admitted that the fit with one resonance, which does not produce such an interesting behavior around 1.9 GeV (dots in Fig. 10), is also acceptable ($\chi^2/NDF = 30.0/36$, C.L.= 74.9%).

E. Cross section drop in the $e^+e^- \to K^+K^-\pi^+\pi^-$

This process is very interesting because the group working on the CMD-3 experiment have recently announced [29] the discovery of a sharp drop of the cross section in the vicinity of the two-nucleon threshold. Not having access to their data, we will search the older data from the *BABAR* [20] and CMD-3 [25] experiments for occurrence of the $\rho(1900)$ resonance.

To describe this process, we use the Lagrangian model assuming the dominance of the $(\phi/\rho^0)K^*\bar{K}^*$ intermediate state. The standard $\phi K^*\bar{K}^*$, $\rho K^*\bar{K}^*$, and $K^*K\pi$ Lagrangians are used together with the VMD Ansatz (3).

1. $K^+K^-\pi^+\pi^-$ in the BABAR experiment

We start with investigating the data by the *BABAR* Collaboration [20] from 2012. To concentrate on the region where the CMD-3 experiment announced this interesting phenomenon, we limit the invariant energy to

$\sqrt{s} \leq 2.02$ GeV, which leaves us with 36 data points. A two-resonance fit with the $\phi(1020)$ and $\phi(1680)$ gives $\chi^2/NDF = 22.8/19$, which translates to C.L.=24.6%. The fit is depicted by the dotted curve in Fig. 11. Including the $\rho(1900)$ decreases χ^2, but because of a smaller
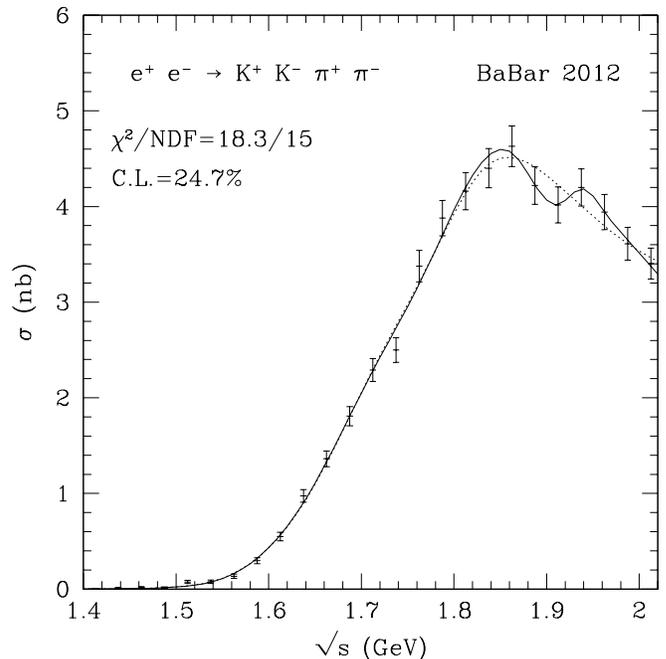

FIG. 11. Cross section of the e^+e^- annihilation into the $K^+K^-\pi^+\pi^-$ system measured by the *BABAR* Collaboration [20]. The Lagrangian-VMD-model fit with two resonances is shown in dots, that with three resonances is depicted by a solid curve.

NDF the quality of the fit remains the same ($\chi^2/NDF = 18.3/15$, C.L.=24.7%). This fit is represented by the solid curve. The mass and width of the $\phi(1020)$ have been fixed at the PDG values [1]. For the $\phi(1680)$ and $\rho(1900)$ we get $M = (1690 \pm 12)$ MeV, $\Gamma = (250 \pm 20)$ MeV and $M = (1906 \pm 15)$ MeV, $\Gamma = (28 \pm 99)$ MeV, respectively. Given the unsatisfactory confidence level, the real errors should be larger. This analysis shows that the *BABAR* data [20] do not require the presence of the $\rho(1900)$ resonance, but can accommodate it.

2. $K^+K^-\pi^+\pi^-$ in the CMD-3 experiment

The CMD-3 experiment in Ref. [25] presented the data from the 2011 and 2012 runs taken at different magnetic fields. Their compatibility is a good test of experimental procedures. To compare our model with the data we proceed in the same way as before. The fit with the $\phi(1020)$ and $\phi(1680)$ gives $\chi^2/NDF = 17.3/30$ (C.L.=96.9%) and is depicted in Fig. 12 by dots. The incorporation of the $\rho(1900)$ noticeably improves the agreement with the data ($\chi^2/NDF = 9.3/26$, C.L.=99.9%, solid curve). Concerning the $\rho(1900)$ parameters, we get $M = (1805 \pm 52)$ MeV,
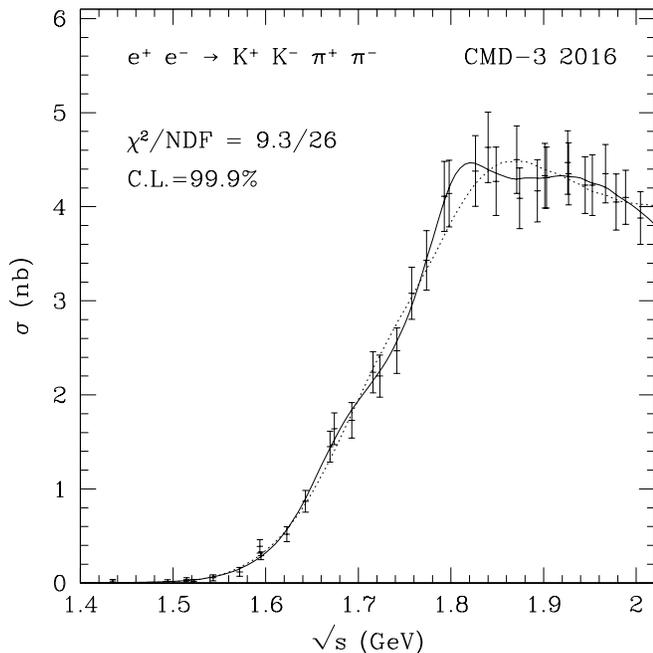
FIG. 12. Cross section of the e^+e^- annihilation into the $K^+K^-\pi^+\pi^-$ system measured in the CMD-3 experiment [25]. The Lagrangian-VMD-model fit with two resonances is shown in dots, that with three resonances is depicted by a solid curve.

$\Gamma = (115 \pm 14)$ MeV. For the $\phi(1680)$, the numbers are $M = (1665 \pm 29)$ MeV, $\Gamma = (140 \pm 41)$ MeV. As the confidence level of the fit without the $\rho(1900)$ is also high, we cannot claim that the presence of the $\rho(1900)$ is required. Certainly, it is not excluded.

F. Cross section dip in the $e^+e^- \rightarrow K^+K^-\pi^0\pi^0$

The *BABAR* Collaboration [20] reported in 2012 on their measurements of the cross section of the $e^+e^- \rightarrow K^+K^-\pi^0\pi^0$ process. Looking at their data in Fig. 13, one immediately notices a dip at about $\sqrt{s} = 1.85$ GeV. Compared to the $K^+K^-\pi^+\pi^-$ case, the dip seems to be in the same position but deeper. It may be the consequence of the interference between two Feynman diagrams originating from the boson (π^0) symmetrization. We start with a two-resonance fit and get quite a good fit ($\chi^2/\text{NDF} = 16.5/20$, C.L.=68.5%) represented in Fig. 13 by the dotted curve. Using the VMD with three resonances (one of them is fixed at the $\phi(1020)$ parameters) we obtain an even better result ($\chi^2/\text{NDF} = 10.4/18$, C.L.=91.8%), shown as a solid curve. The resulting resonance parameters are $M_1 = (1800 \pm 16)$ MeV, $\Gamma_1 = (107 \pm 35)$ MeV, $M_2 = (2376 \pm 38)$ MeV, and $\Gamma_2 = (121 \pm 108)$ MeV. The first resonance resembles the $\rho(1900)$. Because the difference in qualities of the two-resonance and three-resonance fits is not significant, more convincing proof of the dip existence will be possible only after new data are available.
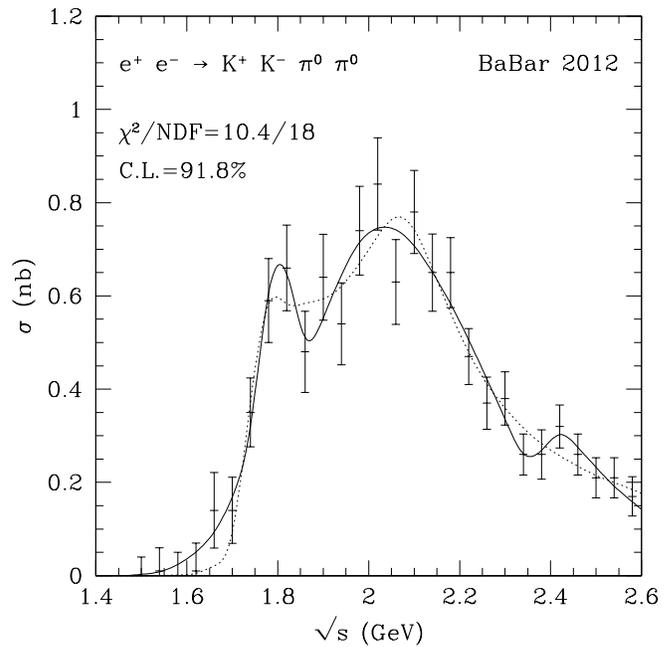

FIG. 13. Cross section of the e^+e^- annihilation into the $K^+K^-\pi^0\pi^0$ system measured by the *BABAR* Collaboration [20]. The Lagrangian-VMD-model fit with two resonances is shown in dots, that with three resonances is depicted by a solid curve.

G. Near-threshold behavior of the $e^+e^- \rightarrow N\bar{N}$

Before discussing the experimental data on the e^+e^- annihilation into the proton-antiproton pair it may be useful to review the result of the quantum electrodynamics about the pointlike Dirac fermions, see, *e.g.*, [47]. It says that at a small s, the cross section is proportional to the center-of-mass system speed β of the outgoing fermion, i.e., it tends towards zero. The Coulomb final-state interaction modifies the cross section. It is described by the Sommerfeld-Gamow-Sakharov factor, see Ref. [48] and references therein. It is

$$T = \eta/[1 - \exp(-\eta)], \qquad (5)$$

where $\eta = \pi\alpha/\beta$. This correction causes the cross section to become a nonzero constant at the threshold. For pointlike protons the threshold value is $\sigma_0 = 0.848$ nb. It is reasonable to assume that for the real protons the cross section at the threshold will not exceed this value.

To construct a VMD model of the e^+e^- annihilation into a nucleon-antinucleon pair, we start from a two-component Lagrangian of the interaction between the ρ field B and the nucleon field ψ

$$\mathcal{L}_{\rho N} = G_{\rho N} \left[\cos\theta_\rho \, j^\mu B_\mu + \frac{\sin\theta_\rho}{m_N} \mathcal{T}^{\mu\nu} G_{\mu\nu} \right], \quad (6)$$

where $j^\mu = \overline{\psi}\gamma^\mu\psi$, $\mathcal{T}^{\mu\nu} = \overline{\psi}\sigma^{\mu\nu}\psi$, and $G_{\mu\nu} = \partial_\mu B_\nu - \partial_\nu B_\mu$. The interaction between the electromagnetic field

A and the ρ field B is given by the Lagrangian $\mathcal{L}_{\rho\gamma} = eg_{\rho\gamma}A^\mu B_\mu$. After a few standard steps, the following expression is obtained for the annihilation cross section

$$\sigma = \frac{4\pi\alpha^2\beta T}{3s}\frac{r_\rho^2}{(s - M_\rho^2)^2 + (M_\rho\Gamma_\rho)^2}\left[\left(1 + 2\frac{m_N^2}{s}\right)\right. \quad (7)$$

$$\times \cos^2\theta_\rho + 12\cos\theta_\rho\sin\theta_\rho + 2\left(\frac{s}{m_N^2} + 8\right)\sin^2\theta_\rho\bigg],$$

where $r_\rho = G_{\rho N}g_{\rho\gamma}$. We have also included the Sommerfeld-Gamow-Sakharov factor T. For a proton it is given by Eq. (5), for a neutron $T = 1$. When fitting the data, r_ρ, θ_ρ, M_ρ, and Γ_ρ will be taken as free parameters. When a fit with more than one resonance is required, the second fraction in (7) is to be replaced by the square of the sum of vector-meson propagators as in (3). This assumes, of course, that the mixing parameter θ is the same for all considered resonances, which may not be true.

A frequently discussed quantity is the ratio of the nucleon form factors. In our model it is given by

$$R = \left|\frac{G_E(s)}{G_M(s)}\right| = \left|\frac{1 + \frac{s}{m_N^2}\tan\theta_\rho}{1 + 4\tan\theta_\rho}\right|. \quad (8)$$

1. $p\bar{p}$ in the CMD-3 experiment

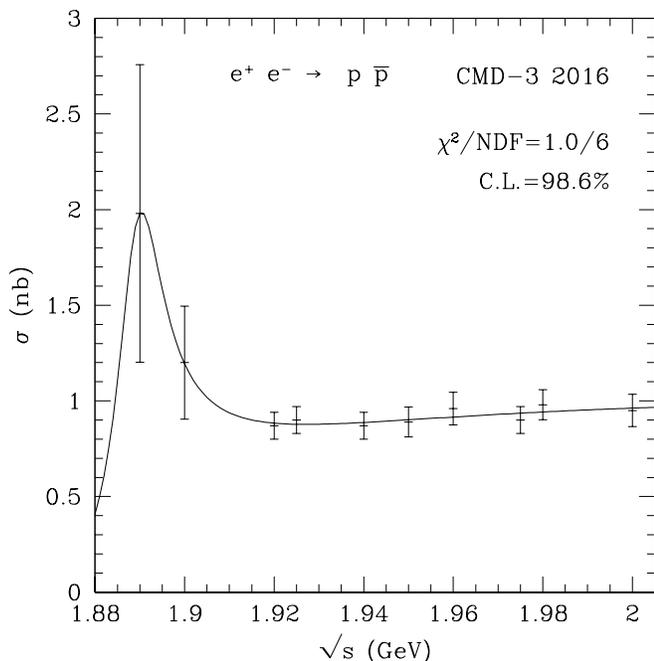The experimental data from the CMD-3 experiment [28], see Fig. 14, contain ten points from the threshold

FIG. 14. Cross section for the $e^+e^- \to p\bar{p}$ process measured by the CMD-3 experiment [28]. The curve represents the fit by the Lagrangian-VMD model with one resonance.

to the highest energy of the VEPP-2000 collider, which

is 2 GeV. This is one of the two examples (for the other, see Sec. III B) in which the $\rho(1900)$ resonance is already clearly visible as a peak before drawing the fitting curve. A one-resonance fit to the data provides the following parameters:

$$M_\rho = (1888.8 \pm 2.4)\text{ MeV},$$
$$\Gamma_\rho = (12 \pm 10)\text{ MeV},$$
$$\theta_\rho = -0.2427 \pm 0.0020,$$
$$r_\rho = (1.88 \pm 0.14)\text{ GeV}^2. \quad (9)$$

The quality of the fit is excellent: $\chi^2/\text{NDF} = 1.0/6$, which implies a confidence level of 98.6 per cent. The CMD-3 data [28] show without any doubt that the observed behavior of the cross section is caused by the coupling of the $p\bar{p}$ pair to the photon through the $\rho(1900)$ resonance. Contrary to the previous surmises, see, e.g., Ref. [21], this resonance does not lie under the $p\bar{p}$ threshold, but well above it. The fitting curve shows it therefore as a perfect peak.

What is very surprising is the behavior of the proton form factor ratio R (8) predicted by our model using the θ_ρ from the fit (9). From the threshold unity the R steeply falls to zero at $\sqrt{s} = 1.886$ GeV and then steeply rises to $R = 12.97$ at $\sqrt{s} = 2$ GeV. There is no experimental evidence yet of such behavior.

2. $p\bar{p}$ by the BABAR Collaboration

The BABAR Collaboration [26] presented their measurement of the $e^+e^- \to p\bar{p}$ cross section from the threshold to $\sqrt{s} = 4.5$ GeV. We want to concentrate on the region close to the threshold. In order to have enough data points for a statistically significant fit, we choose the upper limit somewhat higher than in the CMD-3 case, namely 2.05 GeV. This gives us seven data points. The data and the result of a one-resonance fit using Eq. (7) are shown in Fig 15. The quality of the fit is again excellent: $\chi^2/\text{NDF} = 0.19/3$, C.L.=97.9%. The fit parameters come out as

$$M_\rho = (1885.8 \pm 8.6)\text{ MeV},$$
$$\Gamma_\rho = (12 \pm 16)\text{ MeV},$$
$$\theta_\rho = -0.2452 \pm 0.0037,$$
$$r_\rho = (1.66 \pm 0.11)\text{ GeV}^2, \quad (10)$$

in agreement with the CMD-3 values shown in Eq. (9). Only the value of r_ρ is somewhat smaller, which reflects the difference in overall normalization of the cross sections, visible in Figs. 14 and 15. With θ_ρ from (10) the $\sqrt{s}$-dependence of the $R = |G_E/G_M|$ ratio has a different character than we met in the CMD-3 case. Here, the curve does not touch zero and rises immediately from the threshold. In the whole interval up to 2.0 GeV $|G_M|$ is negligible in comparison with $|G_E|$. Such behavior is not supported by the BABAR data. Fig. 9 in Ref. [26]
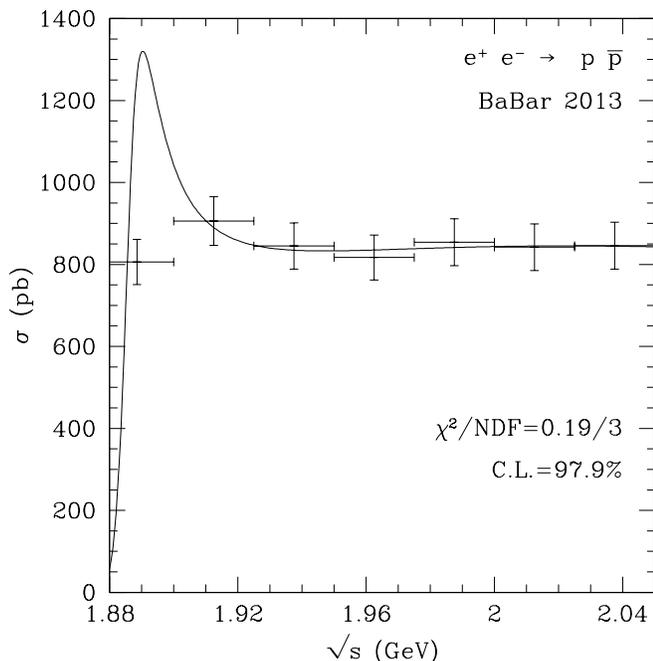
FIG. 15. Cross section for the $e^+e^- \to p\bar{p}$ process measured by the *BABAR* Collaboration [26] and a one-resonance fit using the Lagrangian VMD model.

shows two bins below $\sqrt{s} = 2$ GeV with mean values of r approximately equal to 1.35 and 1.48.

The comparison of Figs. 14 and 15 shows the advantage of the energy scan method over the ISR method in the fine structure measurements not far from the threshold. From the principle of the ISR method it follows that it does not provide the e^+e^- cross section at a given energy, but the mean value of the cross section over a finite energy interval. The fine structure is thus lost. The specifics of the ISR method must be taken into account when fitting the data. In the process of looking for optimal fit parameters we have therefore used Eq. (7) for calculating the average cross sections in the same intervals as in the data and compared them to the experimental values.

The empirical cross section for the $e^+e^- \to p\bar{p}$ process measured by the *BABAR* collaboration [26] can be perfectly fitted by the Lagrangian VMD model (7) with one resonance, the parameters of which are shown in Eq. (10). So, even if the peak is not visible in the data (probably because of their average-in-bin character) we dare to assert that they confirm the character of the $\rho(1900)$ as a narrow resonance lying above the $p\bar{p}$ threshold and coupling to the $p\bar{p}$ pair.

3. $n\bar{n}$ in the SND experiment

The data for the $e^+e^- \to n\bar{n}$ process presented in [27] were accumulated in 2011–2012 at the VEPP-2000 e^+e^- collider in Novosibirsk with the SND detector. The

outcome consists of eleven values of the cross section taken at ten different energies. The experimentalists were faced mainly with problems caused by the cosmic rays background. Nevertheless, their results are in agreement with the FENICE measurements [13] from 1998 and have smaller errors.

We have again fit the SND data using the cross-section formula (7). Our fit is depicted together with the data in Fig. 16. The quality of the fit is a little worse than
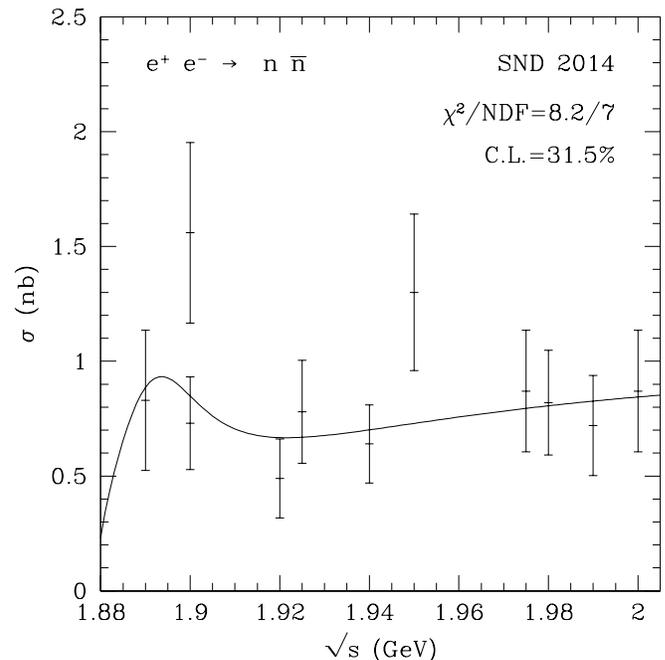

FIG. 16. Cross section for the $e^+e^- \to n\bar{n}$ process measured by the SND experiment [27]. The solid line represents the fit by the Lagrangian-VMD model with one resonance.

in the previous two $p\bar{p}$ experiments, but is still acceptable: $\chi^2/\text{NDF} = 8.2/7$, C.L. = 31.5%.[2] The optimal parameters are

$$M_\rho = (1890.6 \pm 5.2) \text{ MeV},$$
$$\Gamma_\rho = (29 \pm 35) \text{ MeV},$$
$$\theta_\rho = -0.2410 \pm 0.0036,$$
$$r_\rho = (1.92 \pm 0.41)\text{GeV}^2. \qquad (11)$$

They are in perfect agreement with the fit parameters for the CMD-3 (9) and *BABAR* (10) experiments.

Concerning the $|G_E/G_M|$ ratio, it should reach zero at $\sqrt{s} = 1.895$ GeV and then $R = 6.91$ at $\sqrt{s} = 2$ GeV.

The SND experiment gives further support to the notion that the above-threshold behavior of the $N\bar{N}$ cross sections is caused by the coupling of the $p\bar{p}$ and $n\bar{n}$ pairs

---

[2] A better fit with C.L. of 53.1% could be achieved if the two data points at 1.9 GeV were merged to one using the inverse error squared as the weight.

to the narrow resonance $\rho(1990)$, the mass of which lies above the $n\bar{n}$ threshold of 1879.1 MeV. With all three independent $N\bar{N}$ experiments pointing in the same direction the confidence of this notion is very high.

The authors of Ref. [49] recently explained the results of the $N\bar{N}$ experiments [26–28] using nuclear, rather than particle, phenomenology. A quantitative comparison of the success of their model with ours is not possible, as they did not provide any measure of agreement with the data.

4. Common fit to all three $N\bar{N}$ experiments

The ultimate confirmation of the decisive role of the $\rho(1900)$ in the $e^+e^- \to N\bar{N}$ processes together with a more precise determination of its parameters is provided by a common fit to all three $N\bar{N}$ experiments using the formula (7). The quality of the simultaneous fit to the BABAR [26] and CMD-3 [28] $p\bar{p}$ experiments together with the $n\bar{n}$ experiment SND [27] is exceptionally high, characterized by $\chi^2/\mathrm{NDF} = 11.3/22$ and C.L.=97.0%. It not only supports the assertion about a decisive role of the $\rho(1900)$ resonance, but also bears witness to mutual compatibility of the three data sets. The fitted parameters common to all three experiments come out as

$$M_\rho = (1888.3 \pm 2.8) \text{ MeV},$$
$$\Gamma_\rho = (10.0 \pm 4.1) \text{ MeV},$$
$$\theta_\rho = -0.2439 \pm 0.0014. \tag{12}$$

The parameters specific for each of the experiments are $r_\rho(BABAR) = (1.707 \pm 0.055)$ GeV^2, and $r_\rho(\mathrm{CMD\text{-}3}) = (1.787 \pm 0.069)$ GeV^2, $r_\rho(\mathrm{SND}) = (1.75 \pm 0.10)$ GeV^2.

It is interesting that the $\rho(1900)$ width that we determined from the simultaneous analysis of the three experiments is equal to the FENICE's estimate from late 1990's [12, 13]. As concerns the $\rho(1900)$ mass, their central value is about nine MeV below the $n\bar{n}$ threshold, while ours is about nine MeV above that threshold.

IV. SUMMARY AND CONCLUSIONS

Our phenomenological analysis of several e^+e^- annihilation processes suggests that the origin of their special behavior in the vicinity of the $N\bar{N}$ thresholds is the $\rho(1900)$ resonance. Its parameters obtained by fitting the various cross sections are shown in Table III. The most precise values are those obtained from the $p\bar{p}$ [26, 28] and $n\bar{n}$ [27] data. The $\rho(1990)$ masses and widths from those three experiments are mutually compatible and clearly show that the $\rho(1900)$ is not an $N\bar{N}$ resonance because its mass is greater the $n\bar{n}$ threshold.

For some data sets and processes, the quality of the fit was about the same with and without the $\rho(1990)$ resonance. When we also tried to determine the $\rho(1900)$ parameters in these cases, they came out with larger errors

Final state	Data	M (MeV)	Γ (MeV)	Section
$3(\pi^+\pi^-)$	CMD3 '13	1878.3 ± 5.3	24.7 ± 8.7	III A 1
$3(\pi^+\pi^-)$	BABAR '06	1884 ± 29	72 ± 29	III A 2
$2(\pi^+\pi^-\pi^0)$	BABAR '06	1896 ± 60	53 ± 58	III A 3
$2(\pi^+\pi^-\pi^0)$	DM2 '86	1878 ± 40	126 ± 92	III A 4
$3(\pi^+\pi^-)$	DM2 '86	1888 ± 18	44 ± 37	III A 5
$\phi\,\pi^0$	BABAR '08	1906.7 ± 8.8	38 ± 52	III B
$\eta\,\pi^+\pi^-$	SND '18	1812 ± 31	162 ± 70	III C 1
$\eta\,\pi^+\pi^-$	BABAR '07	1831 ± 48	146 ± 167	III C 2
$\eta\,\pi^+\pi^-$	BABAR '18	1879 ± 63	159 ± 137	III C 3
$K^+K^-3\pi$	BABAR '07	1902 ± 26	11 ± 20	III D
$K^+K^-\pi^+\pi^-$	BABAR '12	1906 ± 15	28 ± 99	III E 1
$K^+K^-\pi^+\pi^-$	CMD3 '16	1805 ± 52	115 ± 14	III E 2
$K^+K^-\pi^0\pi^0$	BABAR '12	1800 ± 16	107 ± 35	III F
$p\bar{p}$	CMD3 '16	1888.8 ± 2.4	12 ± 10	III G 1
$p\bar{p}$	BABAR '13	1885.8 ± 8.6	12 ± 16	III G 2
$n\bar{n}$	SND '14	1890.6 ± 5.2	29 ± 35	III G 3
$p\bar{p},\, n\bar{n}$	3 expts.	1888.3 ± 2.8	10.0 ± 4.1	III G 4

TABLE III. Parameters of the resonance influencing the behavior of the e^+e^- annihilation cross section into various final states in the vicinity of $\sqrt{s} = 1.9$ GeV obtained from our fits.

and sometimes "not in line" (see Table III). Obviously, more experimental work is needed to decide about the $\rho(1900)$ involvement in those processes.

A conundrum is why the behavior of the cross sections of some e^+e^- annihilation processes in the vicinity of $\sqrt{s} = 1.9$ GeV is smooth, not influenced by the $\rho(1900)$ resonance. Also here, more experiments are needed to pinpoint those processes. As we cannot expect clarification from nonperturbative Quantum Chromodynamics in the near future, more phenomenological work is also required. A step in this direction was made by Clegg and Donnachie in Ref. [10], where the classification of the six-pion isospin states was done using the correlation numbers scheme of A. Pais [50].

Various versions of the flux-tube breaking model [33, 51] predicted a narrow hybrid vector meson resonance with a mass around 1.9 GeV. This would be one way to explain the "$\rho(1990)$ selection rules". But the nature of the $\rho(1900)$ as a hybrid meson is no longer considered [52].

Important sources of information are the processes, where special behavior occurs when the invariant energy of a produced subsystem (not that of the whole final-state system) approaches 1.9 GeV. Here are a few examples: (i) the diffractive photoproduction of a six-pion system [14, 15]; (ii) the decays $B^\pm \to p\bar{p}K^\pm$ [53] and $\bar{B}^0 \to D^0 p\bar{p}$ [54] with a salient peak just above the $p\bar{p}$ threshold; (iii) a sudden drop near the $p\bar{p}$ threshold in the $\eta'\pi^+\pi^-$ mass distribution in the $J/\psi \to \gamma\eta'\pi^+\pi^-$ decay [55]; (iv) various quarkonia decays with a $p\bar{p}$ pair in the final state, thoroughly listed in Ref. [49].

A simultaneous fit to all processes in which the presence of $\rho(1900)$ is suspected would be valuable, but difficult.

Appendix: The $e^+e^- \to \phi\pi^0$ cross-section: an analytic formula

In Sec. III B we used the Monte Carlo method supplied with the sum of the amplitudes squared to evaluate the cross section of the e^+e^- annihilation into the $\phi\pi^0$ system. Thanks to the binary character of the process it is also possible to get an analytic formula for the cross section. For the reader's convenience we present it here.

Using the standard mesonic Lagrangians [32] and VMD [5] we easily get

$$\sigma(s) = \frac{(\hbar c)^2 \beta}{96\pi s^3} \left[s^3 - (x+3y)s^2 - (x-y)(x+3y)s \right.$$
$$\left. + (x-y)^3 \right] \left| \sum_i \frac{r_i \exp\{\mathrm{i}\delta_i\}}{s - M_i^2 + \mathrm{i}M_i\Gamma_i} \right|^2, \qquad (A.1)$$

where $x = m_\phi^2$, $y = m_{\pi^0}^2$, and β is the ϕ speed in the cms system. To apply an exponential cutoff, the cross section obtained from Eq. (A.1) should be multiplied by function F_{KI}, see Sec. II B. Tests have shown that the analytic formula and the Monte Carlo method give the same results.

[1] M. Tanabashi *et al.* (Particle Data Group), Phys. Rev. D **98**, 030001 (2018).
[2] N.N. Achasov and A.A. Kozhevnikov, Phys. Rev. D **55**, 2663 (1997).
[3] N.N. Achasov and A.A. Kozhevnikov, Phys. Rev. D **58**, 097502 (1998); *ibid.* **62**, 117503 (2000).
[4] N.N. Achasov and A.A. Kozhevnikov, Phys. Rev. D **88**, 093002 (2013).
[5] Y. Nambu and J.J. Sakurai, Phys. Rev. Lett. **8**, 79 (1962), *ibid.* **8**, 191(E) (1962); M. Gell-Mann, D. Sharp, and W. Wagner, Phys. Rev. Lett. **8**, 261 (1962); G.J. Gounaris and J.J. Sakurai, Phys. Rev. Lett. **21**, 244 (1968).
[6] D. Bisello, J.-C. Bizot, J. Buon, A. Cordier, B. Delcourt, and F. Mane, Phys. Lett. B **107**, 145 (1981).
[7] M. Schioppa, Thesis, Universita di Roma "La Sapienza", Rome, 1986.
[8] M.R. Whalley, J. Phys. G **29**, A1 (2003).
[9] R. Baldini-Ferroli: Reported at FENICE Workshop, Frascati, October 1988.
[10] A.B. Clegg and A. Donnachie, Z. Phys. C **45**, 677 (1990).
[11] G. Bardin *et al.*, Nucl. Phys. B **411**, 3 (1994).
[12] B. Antonelli *et al.* (FENICE Collaboration), Phys. Lett. B **365**, 427 (1996).
[13] B. Antonelli *et al.*, Nucl. Phys. B **517**, 3 (1998).
[14] P.L. Frabetti *et al.* (E687 Collaboration), Phys. Lett. B **514**, 240 (2001).
[15] P.L. Frabetti *et al.*, Phys. Lett. B **578**, 290 (2004).
[16] B. Aubert *et al.*, Phys. Rev. D **73**, 052003 (2006).
[17] B. Aubert *et al.*, Phys. Rev. D **77**, 092002 (2008).
[18] B. Aubert *et al.* (BABAR Collaboration), Phys. Rev. D **71**, 052001 (2005).
[19] B. Aubert *et al.*, Phys. Rev. D **76**, 012008 (2007).
[20] J.P. Lees *et al.* (BABAR Collaboration), Phys. Rev. D **86**, 012008 (2012).
[21] R.R. Akhmetshin *et al.*, Phys. Lett. B **723**, 82 (2013).
[22] A.E. Obrazovsky and S.I. Serednyakov, JETP Lett. **99**, 315 (2014).
[23] J. Haidenbauer, C. Hanhart, Xian-Wei Kang, and Ulf-G. Meißner, Phys. Rev. D **92**, 054032 (2015).
[24] V.F. Dmitriev, A.I. Milstein, and S.G. Salnikov, Phys. Rev. D **93**, 034033 (2016).
[25] D.N. Shemyakin *et al.*, Phys. Lett. B **756**, 153 (2016).
[26] J.P. Lees *et al.* (BABAR Collaboration), Phys. Rev. D **87**, 092005 (2013).
[27] M.N. Achasov *et al.*, Phys. Rev. D **90**, 112007 (2014).
[28] R.R. Akhmetshin *et al.*, Phys. Lett. B **759**, 634 (2016).
[29] R.R. Akhmetshin *et al.*, arXiv: 1808.00145 [hep-ex].
[30] N.A. Törnqvist, Z. Phys. C **36**, 695 (1987); **40**, 632(E) (1988); N. Isgur, C. Morningstar, and C. Reader, Phys. Rev. D **39**, 1357 (1989).
[31] N.N. Achasov, S.A. Devyanin, and G.N. Shestakov, Usp. Fiz. Nauk **142**, 361 (1984) [Sov. Phys. Usp. **27**, 161 (1984)].
[32] L. Alvarez-Ruso and V. Koch, Phys. Rev. C **65**, 054901 (2002).
[33] R. Kokoski and N. Isgur, Phys. Rev. D **35**, 907 (1987).
[34] P. Lichard and J. Juráň, Phys. Rev. D **76**, 094030 (2007); J. Juráň and P. Lichard, Phys. Rev. D **78**, 017501 (2008).
[35] N.N. Achasov, S.A. Devyanin, and G.N. Shestakov, Phys. Scr. **27**, 330 (1983).
[36] F. James and M. Roos, Comput. Phys. Commun. **10**, 343 (1975).
[37] F. James, *Monte Carlo Phase Space*, CERN 68-15 (1968).
[38] A. C. Hearn, in *Interactive Systems for Experimental Applied Mathematics*, edited by M. Klerer and J. Reinfelds (Academic Press, New York and London, 1968). See also http://www.reduce-algebra.com/.
[39] M. Benayoun, S.I. Eidelman, V.N. Ivanchenko, and Z.K. Silagadze, Mod. Phys. Lett. A **14**, 2605 (1999).
[40] S. Okubo, Phys. Lett. **5**, 165 (1963); G. Zweig, CERN Report 8419/TH412 (1964); J. Iizuka, Prog. Theor. Phys. Supp. **37**, 21 (1966).
[41] J.P. Lees *et al.* (BABAR Collaboration), Phys. Rev. D **96**, 092009 (2017).
[42] S. Pacetti, Nucl. Phys. A **919**, 15 (2013).
[43] V.M. Aulchenko *et al.*, Phys. Rev. D **91**, 052013 (2015).
[44] M.N. Achasov *et al.*, Phys. Rev. D **97**, 012008 (2018).
[45] B. Aubert *et al.* (BABAR Collaboration), Phys. Rev. D **76**, 092005 (2007), *ibid.* **77**, 119902(E) (2008).
[46] J.P. Lees *et al.* (BABAR Collaboration), Phys. Rev. D **97**,

052007 (2018).

[47] Quang Ho-Kim and Pham Xuan Yem, *Elementary Particles and Their Interactions* (Springer, Berlin 1998), p. 131.

[48] A.B. Arbuzov and T.V. Kopylova, Nucl. Phys. B (Proc. Suppl.) **225-227**, 22 (2012).

[49] A.I. Milstein and S.G. Salnikov, Nucl. Phys. A **977**, 60 (2018).

[50] A. Pais, Ann. Phys. (N.Y.) **9**, 548 (1960).

[51] N. Isgur and J. Paton, Phys. Rev. D **31**, 2910 (1985); T. Barnes, F.E. Close, and E.S. Swanson, *ibid.* **52**, 5242 (1995); P. Page, E.S. Swanson, and A.P. Szczpaniak, *ibid.* **59**, 034016 (1999).

[52] C.A. Meyer and E.S. Swanson, Prog. Part. Nucl. Phys. **82**, 21 (2015).

[53] K. Abe *et al.* (Belle Collaboration), Phys. Rev. Lett. **88**, 181803 (2002).

[54] K. Abe *et al.* (Belle Collaboration), Phys. Rev. Lett. **89**, 151802 (2002).

[55] M. Ablikim *et al.* (BESIII Collaboration), Phys. Rev. Lett. **117**, 042002 (2016).